Linear Analysis of Cross-field Dynamics with Feedback Instability on Detached Divertor Plasmas

Hiroki HASEGAWA[1, 2, *], Hirohiko TANAKA[3] and Seiji ISHIGURO[1, 2]

[1]*National Institute for Fusion Science (NIFS), National Institutes of Natural Sciences (NINS), Toki, Gifu 509-5292 Japan*

[2]*Department of Fusion Science, The Graduate University for Advanced Studies, SOKENDAI, Toki, Gifu 509-5292 Japan*

[3]*Graduate School of Engineering, Nagoya University, Nagoya, Aichi 464-8603 Japan*

[*]Email: hasegawa.hiroki@nifs.ac.jp

Abstract

- The theoretical model of the feedback instability is proposed to explain the mechanism of the correlation between the detachment and the cross-field transport.
- The feedback instability on the detached divertor plasma can be induced in a certain condition in which the recombination frequency is larger than the ion cyclotron frequency in the recombination region. Further the density gradient and the electric field in the direction perpendicular to the magnetic flux surface are not zero in the condition.
- The feedback instability can provide the cross-field plasma transport in the boundary layer of magnetic fusion torus devices.
- The properties of the radial transport observed in the NAGDIS-II linear device experiment are in good agreement with the estimation by the feedback instability model.

1. Introduction

The correlation between the detachment and the cross-field plasma transport in the boundary layer has been reported in various magnetic confinement devices [1-3]. Such a correlation is expected to expand the width of the peak flux to the divertor target. However, the physical dynamics of the correlation has not been revealed. On the other hand, the detached divertor plasma can be considered as the coupling of two magnetized plasmas characterized by different current mechanisms. Such a coupling system is also found in the space plasma as the magnetosphere-ionosphere (M-I) coupling. The electric current in the magnetosphere streams along the geomagnetic field line, while that in the ionosphere can flow in the direction perpendicular to the geomagnetic field because the frequency of collision between ions and neutrals ν_{in} is larger than the ion cyclotron frequency Ω_{ci}. This difference of the current mechanism between the magnetosphere and the ionosphere can induces the instability called "feedback instability" [4]. The field-aligned current (FAC) and the ionosphere plasma density grow locally by the feedback instability and auroral arcs are formed in the region where FAC is enhanced [5].

In this study, we investigate the cross-field dynamics in the detached plasma state with the coupling model between magnetized plasmas characterized by different current mechanisms as described above. In the recombination region in front of a divertor target, the recombination frequency ν_{rec} can be larger than Ω_{ci} because of the high density and the low temperature. In such a situation, the cross-field motion of ions is mainly in the direction of the electric field, while that of electrons is almost in the direction of the ***E***×***B*** drift. Thus, the difference in the direction of motion may provide the cross-field current in the recombination region (see **Fig. 1**). On the other hand, the cross-field current can be generated by only the polarization, the grad-*B* and the diamagnetic drifts in the upstream plasma. We have considered whether such a difference between the current mechanisms in each region induces the cross-field plasma transport.

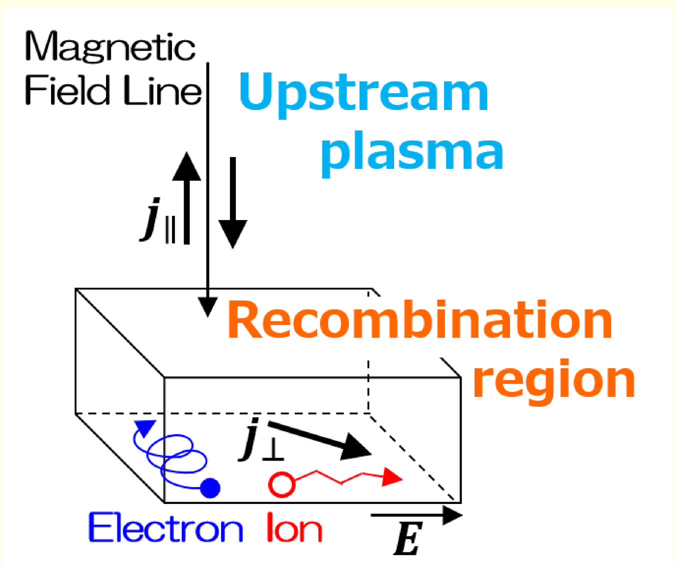

Figure 1: Schematic diagram of the detached divertor plasma from the viewpoint of the coupling model.

2. Configuration and Equations

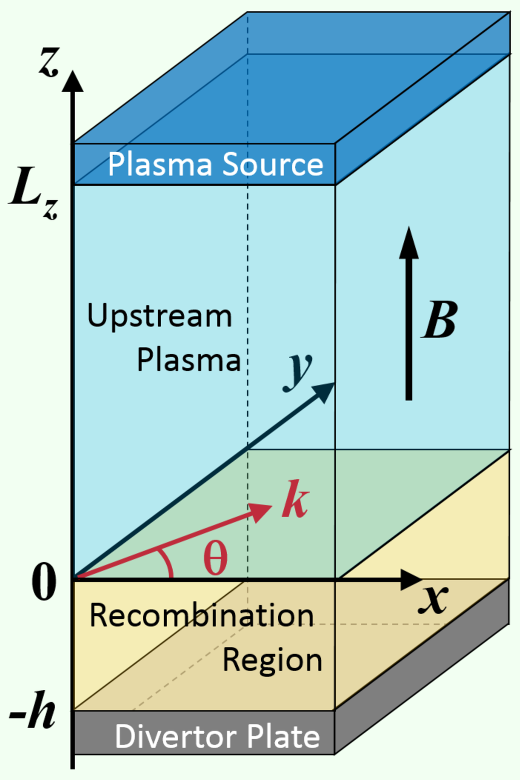

Figure 2: Configuration of the system for the theoretical model.

For derivation of the linear dispersion relation, we use the continuity equations for electron and ion and the charge conservation equations in each region:

$$\frac{\partial n^{\mathrm{P}}}{\partial t} + \nabla_\perp\cdot\left(n^{\mathrm{P}}\boldsymbol{v}^{\mathrm{P}}_{s\perp}\right) + \frac{\Gamma^{\mathrm{PS}}_{s\parallel}-\Gamma^{\mathrm{B}}_{s\parallel}}{L_z} = 0$$

$$\nabla_\perp\cdot\boldsymbol{j}^{\mathrm{P}}_\perp + \frac{j^{\mathrm{PS}}_\parallel - j^{\mathrm{B}}_\parallel}{L_z} = 0$$

$$\frac{\partial n^{\mathrm{R}}}{\partial t} + \nabla_\perp\cdot\left(n^{\mathrm{R}}\boldsymbol{v}^{\mathrm{R}}_{s\perp}\right) + \frac{\Gamma^{\mathrm{B}}_{s\parallel}-\Gamma^{\mathrm{DP}}_{s\parallel}}{h} = -\alpha\left[\left(n^{\mathrm{R}}\right)^2 - \left(n^{\mathrm{R}}_0\right)^2\right]$$

$$\nabla_\perp\cdot\boldsymbol{j}^{\mathrm{R}}_\perp + \frac{j^{\mathrm{B}}_\parallel - j^{\mathrm{DP}}_\parallel}{h} = 0$$

P: upstream plasma, R: recombination region, B: boundary between "P" and "R" (z = 0), PS: plasma source ($z = L_z$), DP: divertor plate ($z = -h$) (see **Fig. 2**), s: particle species, 0: equilibrium state and α: recombination coefficient.

The fluid velocities in each region are given by

$$\boldsymbol{v}^{\mathrm{P}}_{s\perp} = \frac{\boldsymbol{E}^{\mathrm{P}}_\perp\times\boldsymbol{B}}{B^2} - \frac{m_s}{q_sB^2}\left(\frac{\partial}{\partial t}+\boldsymbol{v}^{\mathrm{P}}_{s\perp}\cdot\nabla_\perp\right)\left(\nabla_\perp\phi^{\mathrm{P}}\right) + \frac{T^{\mathrm{P}}_s}{q_sB^2}\frac{\partial B}{\partial x}\boldsymbol{y} + \frac{T^{\mathrm{P}}_s}{q_sBn^{\mathrm{P}}}\left(\frac{\partial n^{\mathrm{P}}}{\partial x}\boldsymbol{y} - \frac{\partial n^{\mathrm{P}}}{\partial y}\boldsymbol{x}\right)$$

$$\boldsymbol{v}^{\mathrm{R}}_{s\perp} = \mu_{\mathrm{Hs}}\left[\frac{\boldsymbol{E}^{\mathrm{R}}_\perp\times\boldsymbol{B}}{B} - \frac{m_s}{q_sB}\left(\frac{\partial}{\partial t}+\boldsymbol{v}^{\mathrm{R}}_{s\perp}\cdot\nabla_\perp\right)\left(\nabla_\perp\phi^{\mathrm{P}}\right) + \frac{T^{\mathrm{R}}_s}{q_sB}\frac{\partial B}{\partial x}\boldsymbol{y} + \frac{T^{\mathrm{R}}_s}{q_sn^{\mathrm{R}}}\left(\frac{\partial n^{\mathrm{R}}}{\partial x}\boldsymbol{y} - \frac{\partial n^{\mathrm{R}}}{\partial y}\boldsymbol{x}\right)\right] + \frac{q_s}{|q_s|}\mu_{\mathrm{Ps}}\boldsymbol{E}^{\mathrm{R}}_\perp$$

where μ_{Hs} and μ_{Ps} are Hall and Pedersen mobilities defined by

$$\mu_{\mathrm{Hs}} = \frac{|q_s|}{m_s\nu_{\mathrm{rec}}}\frac{\Omega_{cs}/\nu_{\mathrm{rec}}}{1+(\Omega_{cs}/\nu_{\mathrm{rec}})^2} \quad \text{and} \quad \mu_{\mathrm{Ps}} = \frac{|q_s|}{m_s\nu_{\mathrm{rec}}}\frac{1}{1+(\Omega_{cs}/\nu_{\mathrm{rec}})^2}$$

The equilibrium and boundary conditions are shown in the preprint.

3. Linear Dispersion Relation

Linearizing the equations mentioned above, we obtain the linear dispersion relation;

$$\omega^3 + A_2(k,\theta)\,\omega^2 + A_1(k,\theta)\,\omega + A_0(k,\theta) = 0$$

The details of each coefficient are described in the preprint.

3.1. Typical Fusion Torus Case

The one mode of the dispersion relation becomes unstable for the typical fusion torus case as shown in **Fig. 3**:

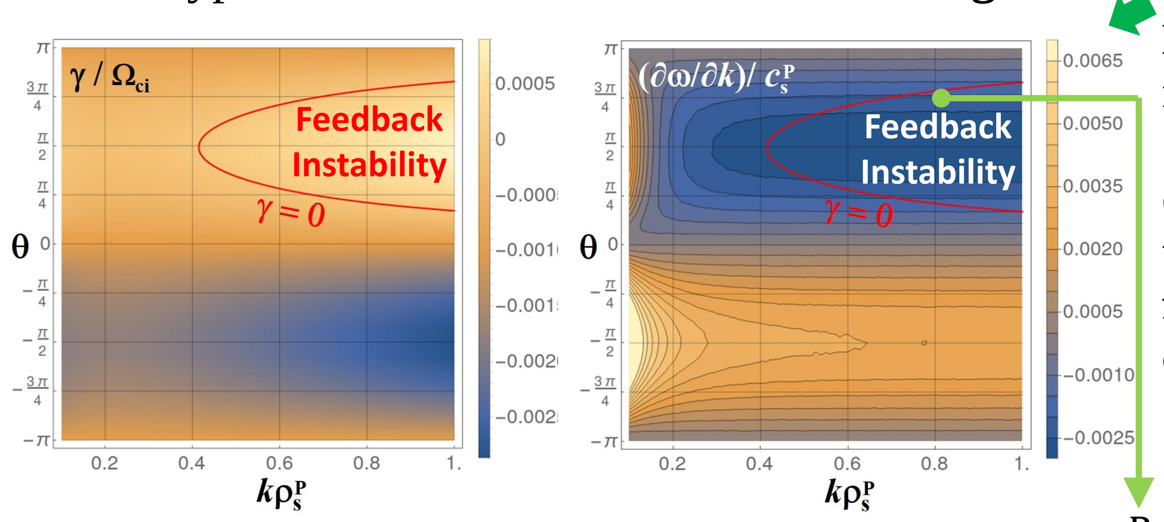

Figures 3 & 4: Dependences of the growth rate γ and the group velocity ∂ω/∂k of the unstable mode on the wave number *k* and the propagation direction θ for the typical fusion torus case.

The plasma can be transported with the speed ~ $0.002\ c^{\mathrm{P}}_s$. Here, c_s is the ion acoustic speed.

The estimation as mentioned in **Fig. 5** shows the heat flux density reduction:

$$1 - (v_{gx}/c^{\mathrm{R}}_s)(\tilde{n}/n^{\mathrm{R}}_0)(h/\lambda^{\mathrm{B}}_{\mathrm{q}}) \approx 82\ \%,$$

the heat flux width expansion: $1 + (h/\lambda^{\mathrm{B}}_{\mathrm{q}})(v_{gx}/c^{\mathrm{R}}_s) \approx 280\ \%$.

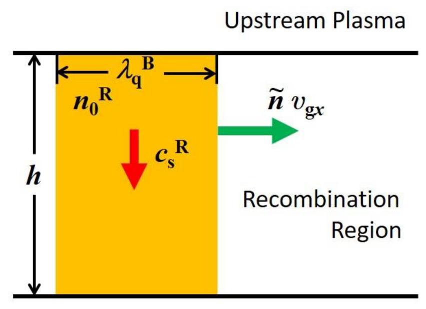

Figure 5: Schematic diagram for the estimations of the heat flux density reduction and the heat flux width expansion.

3.2. NAGDIS-II Linear Device Case

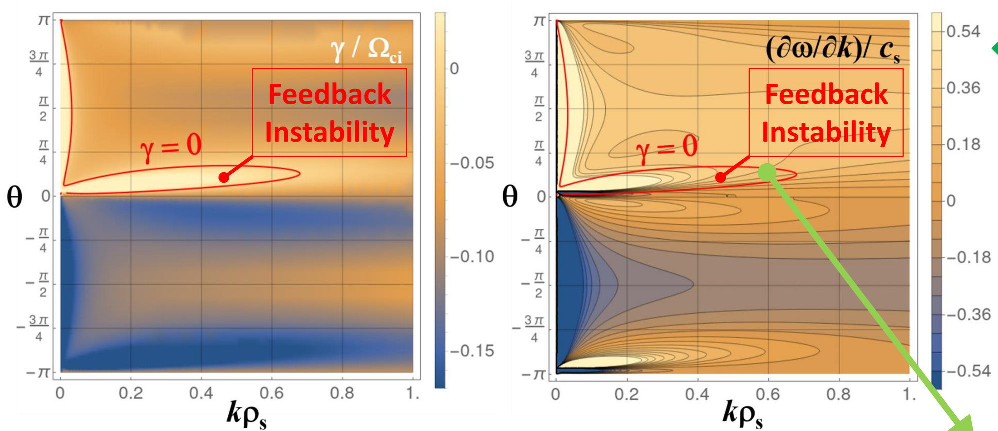

Figures 6 & 7: Dependences of the growth rate γ and the group velocity ∂ω/∂k of the unstable mode on the wave number *k* and the propagation direction θ for the NAGDIS-II linear device case.

The plasma can be transported with the speed ~ $0.2\ c^{\mathrm{P}}_s$, that is, with v_{gx} ~ 800 m/s and v_{gy} ~ 200 m/s.

Figure 8: Comparison with the NAGDIS-II experiment.

This estimation is in good agreement with the radial speed v_r ~ 80 [m/s] at r ~ 20 [mm] and azimuthal speed v_θ ~ 200 [m/s] at r ~ 5 [mm] obtained for the spiralling plasma ejection in the experiment if v_r is reduced as r increases (see **Fig. 8**).

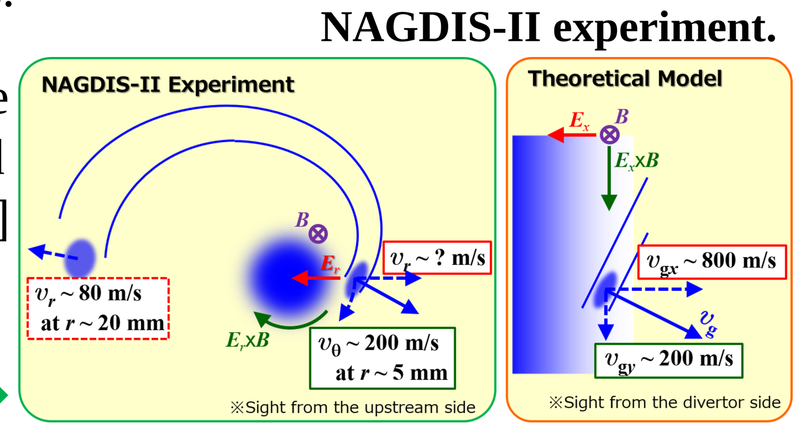

4. Summary and Future Works

- The **linear dispersion relation** for the detached plasma has been derived with the coupling model between the magnetized plasmas characterized by different current mechanisms in the simple configuration.
- The **unstable mode** has been found from the dispersion relation under a certain condition for both the typical fusion torus case and the NAGDIS-II linear device case.
- The **heat flux density reduction** and the **heat flux width expansion** provided by the unstable waves have been estimated for the typical fusion torus case.
- The transport property estimated by the proposed model is in good **agreement with** that of the spiralling plasma ejection observed in the **NAGDIS-II experiment**.
- In future works, we plan to consider the situations including the temperature fluctuation and the spatial variations in the magnetic field direction and perform the non-linear simulation.

Acknowledgment

This work is performed with the support and under the auspices of the NIFS Collaboration Research programs (NIFS19KNSS119, NIFS21KNSS155, NIFS17KNXN342, NIFS20KNSS136, NIFS19KNXN391, NIFS19KUGM140, NIFS20KNSS136, NIFS19KNTT052, NIFS21KNTT060, NIFS19KNTS058, NIFS21KNTS071 and NIFS19KNTS060), supported by the NINS program of Promoting Research by Networking among Institutions (Grant Number 01421701) and supported by JSPS KAKENHI Grant Numbers JP19K03787 and JP16H06139.

References

[1] S. Potzel *et al*., J. Nucl. Mater. **438** (2013) S285.
[2] H. Tanaka *et al*., Phys. Plasmas **17** (2010) 102509.
[3] H. Tanaka *et al*., Plasma Phys. Control. Fusion **60** (2018) 075013.
[4] Tetsuya Sato, J. Geophys. Res. **83** (1978) 1042.
[5] Hiroki Hasegawa, Nobuaki Ohno and Tetsuya Sato, J. Geophys. Res. **115** (2010) A08304.